

Julian Wang
Donglu Shi
Yehao Song *Editors*

Advanced Materials in Smart Building Skins for Sustainability

From Nano to Macroscale

Advanced Materials in Smart Building Skins for Sustainability

Julian Wang · Donglu Shi · Yehao Song
Editors

Advanced Materials in Smart Building Skins for Sustainability

From Nano to Macroscale



Springer

Editors

Julian Wang 

Department of Architectural Engineering
and Department of Architecture
Pennsylvania State University
University Park, PA, USA

Donglu Shi

Department of Mechanical and Materials
Engineering
University of Cincinnati
Cincinnati, OH, USA

Yehao Song

School of Architecture
Tsinghua University
Beijing, China

ISBN 978-3-031-09694-5

ISBN 978-3-031-09695-2 (eBook)

<https://doi.org/10.1007/978-3-031-09695-2>

© The Editor(s) (if applicable) and The Author(s), under exclusive license to Springer Nature Switzerland AG 2023

This work is subject to copyright. All rights are solely and exclusively licensed by the Publisher, whether the whole or part of the material is concerned, specifically the rights of translation, reprinting, reuse of illustrations, recitation, broadcasting, reproduction on microfilms or in any other physical way, and transmission or information storage and retrieval, electronic adaptation, computer software, or by similar or dissimilar methodology now known or hereafter developed.

The use of general descriptive names, registered names, trademarks, service marks, etc. in this publication does not imply, even in the absence of a specific statement, that such names are exempt from the relevant protective laws and regulations and therefore free for general use.

The publisher, the authors, and the editors are safe to assume that the advice and information in this book are believed to be true and accurate at the date of publication. Neither the publisher nor the authors or the editors give a warranty, expressed or implied, with respect to the material contained herein or for any errors or omissions that may have been made. The publisher remains neutral with regard to jurisdictional claims in published maps and institutional affiliations.

This Springer imprint is published by the registered company Springer Nature Switzerland AG
The registered company address is: Gewerbestrasse 11, 6330 Cham, Switzerland

Preface

Today's nanotechnologies and advanced materials have rapidly advanced into many areas, particularly in civil engineering and architectural design for the development of responsive and adaptive structures which are not only for providing occupant comfort but also for achieving building energy efficiency and sustainable environmental performance. The concept of "smart" building skins has emerged that can respond to any environmental changes, especially involving energy sources and health factors. These environmental changes can trigger a "response" manifested by a material property that can be readily measured and translated to other variables for required functionalities and applications. In this fashion, a building skin is no longer a passive physical barrier but structurally transformed into an active device system capable of multifunctional energy and environmental performances such as energy harvest and CO₂ reduction. For instance, the smart building skin can now be engineered for solar harvesting, conversion, and utilization as in the so-called Building Integrated Photovoltaic (BIPV). In BIPV, the high-rise building skins provide ideal transparent substrates for energy device architecture based on nanoscale thin films. The smart building concept has paved a new path to energy-neutral civic infrastructures that will have high societal impacts on energy conservation, public health, prosperity, and welfare.

This book is a collection of chapters that focus on key areas of smart building skins embodied in the novel advanced materials with unique structures and properties that enable multiple functions in energy efficiency, solar harvesting, and environmental greenness. These chapters provide the most up-to-date research outcomes on novel materials synthesis, structure characterization, device architecture, and their novel applications in smart building skins. The topics of these chapters cover broad interdisciplinary areas including nanotechnology, materials science, energy devices, architecture, urban planning, and civil engineering. In particular, new trends in modern architectural design are introduced with consideration of energy conservation, environmental greenness, and net-zero. All chapters are developed by experts in different fields who have been collaboratively conducting research about energy-efficient building skins.

Chapters 1–5 concentrate on the design, characteristics, development, fabrication, and performance analysis of *advanced materials*, taking the consideration of building-integrated application paradigms. The introduced materials range from nanoscale spectral selective materials to molecular scale programmable biological materials, and architectural scale wooden materials/structures. Spurred by the introduction of various new materials, Chapters 6–9 deal with *engineering solutions and technologies* to incorporate advanced materials and investigate their impacts, such as the envelope thermal engineering with smart materials, building-integrated photovoltaic technologies and their influences on microclimates, and computational technologies for energy analysis of dynamic building skins. Chapters 10–13 take the perspective of *architectural design*, illustrating and demonstrating new methodologies, processes, models, and practical principles for integrating dynamic envelopes consisting of advanced materials into the architectural scale, with considerations of material design knowledge transfer, environmental interactions, esthetics, and user testing.

We have organized this book to provide overviews of key issues on the novel applications of advanced materials in architecture that are tailored to multifunctional, energy-efficient, environmentally green building skins. All chapters are developed in a tutorial fashion for technical specialists in a variety of fields such as materials science, mechanical engineering, civil engineering, and architectural design. This book is expected to have a large readership suitable for both academic and industrial researchers, including graduate and undergraduate students, scholars, engineers, and practitioners in sustainable design and building façade engineering.

We are most grateful to all authors for contributing their most valuable works to this book. The assistance of editor Madanagopal Deenadayalan from Springer for formatting this book is very much appreciated.

University Park, USA
Cincinnati, USA
Beijing, China

Julian Wang
Donglu Shi
Yehao Song

Contents

1	Spectral Selective Solar Harvesting and Energy Generation via Transparent Building Skin	1
	Jou Lin, Mengyao Lyu, Yuxin Wang, Brent Webster, and Donglu Shi	
2	Low Energy Adaptive Biological Material Skins from Nature to Buildings	59
	Laia Mogas-Soldevila	
3	Dynamic Electro-, Mechanochromic Materials and Structures for Multifunctional Smart Windows	73
	Yao Zhao, Yanbin Li, and Jie Yin	
4	Material Programming for Bio-inspired and Bio-based Hygromorphic Building Envelopes	99
	Dylan Wood, Tiffany Cheng, Yasaman Tahouni, and Achim Menges	
5	Solar-Thermal Conversion in Envelope Materials for Energy Savings	113
	Mohammad Elmi and Julian Wang	
6	Thermally Responsive Building Envelopes from Materials to Engineering	129
	Hongyu Zhou and Yawen He	
7	Energy Performance Analysis of Kinetic Façades by Climate Zones	149
	Chengde Wu	
8	Integration of Solar Technologies in Facades: Performances and Applications for Curtain Walling	167
	Paolo Rigone and Paolo Giussani	
9	Interdependencies Between Photovoltaics and Thermal Microclimate	189
	Elisabeth Fassbender and Claudia Hemmerle	

10 Material Driven Adaptive Design Model for Environmentally-Responsive Envelopes	207
Maryam Mansoori, Zofia Rybkowski, and Negar Kalantar	
11 Design Principles, Strategies, and Environmental Interaction of Dynamic Envelopes	221
Pengfei Wang, Junjie Li, and Zehui Peng	
12 Aesthetics and Perception: Dynamic Facade Design with Programmable Materials	243
Dale Clifford	
13 Design Research on Climate-Responsive Building Skins from Prototype and Case Study Perspectives	257
Zhenghao Lin and Yehao Song	
Index	277

Chapter 1

Spectral Selective Solar Harvesting and Energy Generation via Transparent Building Skin



Jou Lin, Mengyao Lyu, Yuxin Wang, Brent Webster, and Donglu Shi

Abstract Today's nanoscience has rapidly advanced into many areas of engineering, particularly in architectural design of building skins for the development of environmentally responsive structures. Not only does this improve occupant comfort, but also increases energy sustainability. Recently, advanced materials have been utilized for developing large-scale building skins with intelligent functionalities. Many current challenges focus on improving environmental safety, increasing energy efficiency, and reducing our carbon footprint. Advanced materials have played key roles in addressing these critical issues through fascinating properties that are ideal for building skin engineering. In this chapter, a series of bio-inspired green nano hybrids are introduced for solar harvesting, energy generation, and photothermally-activated building heating. These nano biohybrids can be physically retrofitted into existing residential buildings and structures, independently providing self-sustainable green energy. This chapter explores the most recent developments of nanostructure-based building skins that are smart, intelligent, adaptive, responsive and biologically inspired for energy and environmental sustainability. More specifically, we have developed smart building façades utilizing nanomaterial assemblies that have the ability to regulate and control energy consumption and generation, leading to energy neutral civic infrastructure. Novel nanostructures are designed, synthesized, and developed capable of the most efficient solar harvesting and energy generation. Fundamental studies have been carried out to identify operating mechanisms dictating the optical, thermal, and electrical properties of the thin films on building skins for required functions. Lab-scale modules can be designed to test the performance of multifunctional thin films in terms of solar harvesting, visible transmittance, photovoltaic (PV) and photothermal (PT) efficiencies. The novel concepts include Optical Thermal Insulation (OTI) without any intervention medium typically used in glazing technologies, and building skins with PV-PT dual modalities that can be seasonably altered for energy efficiency and generating solar-mediated thermal energy for building heating utilities. OTI is established by solar heating of a

J. Lin · M. Lyu · Y. Wang · B. Webster · D. Shi (✉)

The Materials Science and Engineering Program, Department of Mechanical and Materials Engineering, College of Engineering and Applied Science, University of Cincinnati, Cincinnati, OH 45221, USA

e-mail: shid@ucmail.uc.edu

photothermal coating on a window surface. by reducing the temperature difference between the window surface and room interior, the heat loss through a single pane is lowered without the air gap of the double pane. A transparent building skin can be engineered as a PV and PT device in the same surface coating with a dual modality. While the solar energy harvested can be converted to electricity via PV in the summer, the same film is photonically-activated to generate heat in the winter for reduced heat loss. The PV-PT dual-modality device can be applied as a smart building skin upon a large surface area for enhanced solar harvesting and alternative energy generation such as electrical and thermal energy. The solar light can also be wave-guided through transparent photo-thermal panels for generating high heat for building utilities. This chapter will devote much of its portions to describing the fundamental mechanisms of these new concepts as well as the engineering implementations in building skin architecture.

Keywords Advanced materials · Nano technology · Smart building skin · Nanobiohybrids · Spectral selective · Photothermal · Photovoltaic · Energy sustainability

1.1 Introduction

1.1.1 *Optical Thermal Insulation via Photothermal Window Coatings*

The residential and commercial building sectors accounted for about 40% (or about 40 quadrillion British thermal units) of the total U.S. energy consumption in 2018 (Arasteh et al., 2006). Therefore, there is an increasing need to develop lighter material structures (such as single pane) and energy efficient building skins. One of the key issues deals with overall building energy and material consumption including electricity, heating and cooling, and materials production due to large building sizes. Recent advancements in technology have enabled glass to be integral of both the interior and exterior architecture making it a major component of building façades (Fig. 1.1). However, great challenges remain in terms of thermal transfer, energy efficiency and lighting requirements, especially heat loss in cold climate. Although various glazing technologies have been developed including low emissivity coatings and double/triple panes, a huge consumption of energy will not be resolved until fundamentally different concepts and engineering innovations are developed.

For instance, the current technology for efficient windows relies upon the double-pane insulated glass unit (IGU) with a low-emissivity (low-e) coating. Although the double-pane IGU may meet some of the requirements in energy consumption, the single-pane windows will be highly desirable for obvious reasons including lighter weight, straightforward manufacturing, and less materials needed. The advanced single pane IGUs may ultimately replace double panes with similar performance characteristics. However, a key challenge in developing the single-pane IGUs is the



Fig. 1.1 Typical modern building with glass facades

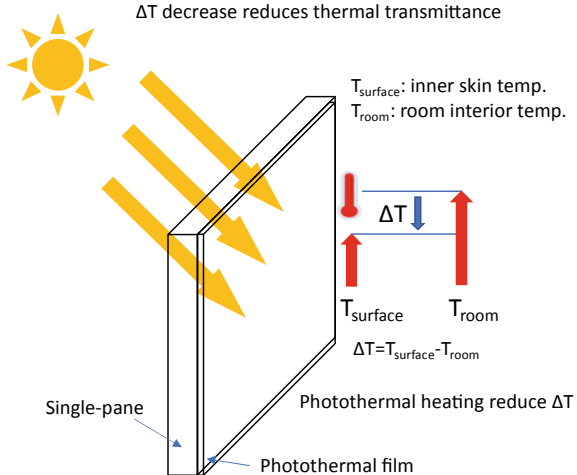
thermal insulation without the air gap between the double panes. As air is well known for its low thermal conductivity, few materials can be used to replace air except heavier gases such as argon. There are two main aspects in the design of a single-pane IGU: (1) replace the air gap with a novel insulator so that the thermal conductivity no longer depends on the air gap spacing (i.e. double panes), and (2) replace the low emissivity coating with a new reflection system that can efficiently block the heat loss from the interior where the heating source exists.

The basic criterion for a thermally well-insulated single-pane window is the U-factor according to Energy Star certification in colder regions of the US (Environmental Protection Agency, 2015). The single-pane IGU will have to meet the following conditions: (1) a single pane without air spacing; (2) the U-factor for an entire window needs to be less than 0.30 (Environmental Protection Agency, 2015; U. E. P. Agency, 2018; Carmody et al., 2007); (3) a single-pane IGU with sufficiently high interior temperate allowing a 30% relative humidity for external temperature of -0°C , and (4) a low emissivity coating that can selectively and efficiently reflect the thermal energy generated from the heating source. In order to meet these conditions, advanced materials will play key roles in many aspects of engineering design, optical and thermal property characterization, and architectural integration into the building structure. The current advancement of nanotechnologies will enable design, development and manufacture of new single panes that are thermally highly insulating, optically transparent, visually finesse, and energy efficient.

The goal in developing energy-efficient building skins is to achieve the same level of thermal insulation of conventional glazing technologies by using single panes without any thermal intervention medium, such as air or argon. However, this critical issue cannot be easily addressed by only relying on identifying insulating materials since most of the thermal insulators are either nontransparent or opaque, thus not

Fig. 1.2 Concept of optical thermal insulation

Optical Thermal Insulation

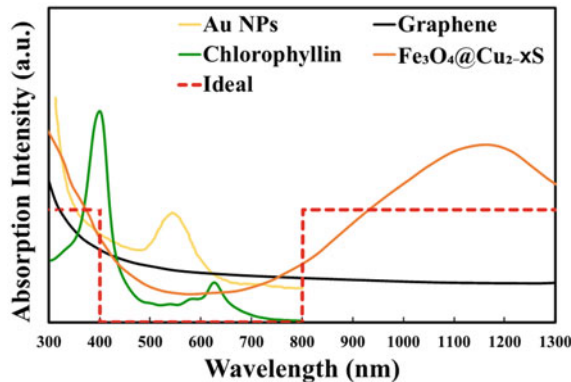


suitable for window applications. Recently, a novel concept of Optical Thermal Insulation (OTI) has been developed by solar heating of the window surface through a nano-scale thin film coating (Fig. 1.2) (Lin et al., 2020). Thermal losses can be significantly reduced if the window surface temperature is raised to the level approaching that of the room interior (Fig. 1.2). In this way, double panes will not be needed to reduce the heat loss, therefore saving tremendous energy and insulation materials.

The optical thermal insulation is achieved by developing a transparent photothermal film deposited on the window surface which can rapidly heat up under solar light irradiation. The thin film is designed, synthesized, and tailored to selectively absorbing solar light in the ultraviolet (UV) and near infrared (NIR) regions for converting these photon energies to thermal heat, leading to window surface temperature increase. For window applications, the film has to be rendered highly transparent. This requires manipulation of the optical properties of the thin films with high Average Visible Transmittance (AVT).

Figure 1.3 shows the absorption spectra for various materials as indicated (Tian et al., 2013; Zhao et al., 2019a). As can be seen in this figure, while gold nanoparticles exhibit strong absorption below 300 nm, there is another peak at 520 nm, contributing to considerable visible light absorption. Much stronger absorption is observed in the UV range for graphene and Fe_3O_4 nanoparticles, but they gradually decay to the minimum in the visible range up to Near-Infrared (NIR). Therefore, all conducting materials with high charge densities exhibit strong photothermal effects but lacking sufficient visible transmittance. However, chlorophyll shows a saddle-like spectrum with two peaks respectively at 400 nm (blue-violet) and 700 nm (NIR), which is consistent with its green color. It is this typical spectrum with a saddle-like shape that qualifies chlorophyll for transparent building skin application. As can also be seen in Fig. 1.3, $\text{Fe}_3\text{O}_4 @ \text{Cu}_{2-x}\text{S}$ is characterized with a "U" shaped spectrum showing strong

Fig. 1.3 Spectra of various photothermal materials



IR absorption extending to 1500 nm or even further (the peak is around 1200 nm). The dashed line in Fig. 1.3 represents an idealized optical characteristic with step-function like UV and IR absorptions and high visible transmittance for single-pane applications.

Based on the optical properties shown in Fig. 1.3, materials with either “U-shaped” or “saddle-like” absorption characteristics may meet the requirements in single-pane designs. Both iron oxides and porphyrin compounds are ideal materials for photothermal coatings in energy-efficient building skin applications. The porphyrin compounds such as chlorophyll and chlorophyllin share very similar structures of the porphyrin rings with the only difference in the metal atom at the ring center. Chlorophyll has a center magnesium atom; replacing it with a copper atom results in chlorophyllin. Both are highly abundant in nature and environmentally green.

Absorption behavior of Fe_3O_4 nanoparticles can be modified by coating the particle surfaces with CuS, forming a core–shell nanostructure in $\text{Fe}_3\text{O}_4@\text{Cu}_{2-x}\text{S}$ that exhibits much stronger near-infrared absorptions as shown in Fig. 1.3 (Tian et al., 2013) The thin films of both porphyrins and iron oxides can be spin-coated on glass substrates with 500 nm thickness achieving an average visible transmittance above 90%. Upon irradiation with simulated solar light, the surface temperature can rapidly increase as shown in Fig. 1.4a for $\text{Fe}_3\text{O}_4@\text{Cu}_{2-x}\text{S}$, which contributes to the optical thermal insulation by reducing the temperature difference between the window surface and room interior (Fig. 1.1). Similar heating curves have been obtained for chlorophyll (Fig. 1.4b) and chlorophyllin films (Fig. 1.4c). The current research has been focused on improving both heating efficiency and AVT in the PT coatings for OTI applications.

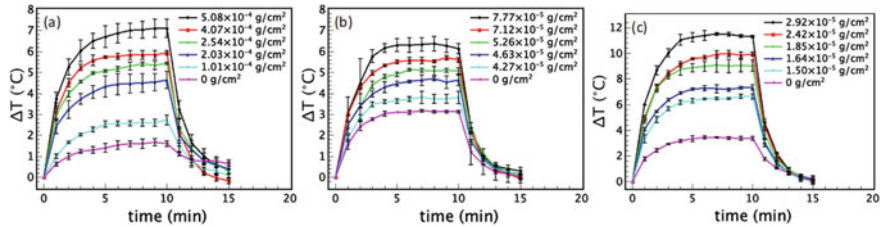


Fig. 1.4 Heating curves of **a** $\text{Fe}_3\text{O}_4@\text{Cu}_{2-x}\text{S}$, **b** chlorophyll, and **c** chlorophyllin thin films

1.1.2 Photovoltaic and Photothermal Dual-Modality Building Skins

Harvesting solar energy for various applications has been an intense research area, especially in photovoltaic solar cells. Interestingly both transparent photo-thermal (TPT) and transparent photovoltaic (TPV) films share a common spectral characteristic requirement: high visible transmittance (AVT) for visible transparency. However, TPT requires high absorptions in both UV and NIR bands, while only UV is preferred for TPV since IR heating results in considerable efficiency decrease (Effect of Temperature, 2021; Bjørk & Nielsen, 2015). Another important common feature of TPV and TPT lies on a large surface area requirement for efficient solar light harvest. As noted above, the current glass building skin is characterized with entire building surfaces, particularly large for high-rises. Take both advantages of free solar light and huge building surfaces, the so-called building integrated photovoltaic (BIPV) has been extensively researched and developed. However, it is possible to further increase the energy efficiency of a building skin by incorporating both TPV and TPT via the concept of PV-PT dual modality that can most efficiently harvest solar light and convert it to two forms of energy: thermal and electric energy, which can be alternated seasonably. This is highly possible if a novel transparent film on glass building skin surface can be engineering to have both PT and PV properties (Lin & Shi, 2021).

The concept of the photo-thermal-photovoltaic (PT-PV) dual-modality assembly is schematically illustrated in Fig. 1.5. As shown in this figure, the PT-PV film is featured with several key characteristics: (1) it is highly transparent but only absorbing UV and NIR for energy conversion; (2) upon absorbing solar light in the UV and NIR regions, energy conversion seasonably takes two paths: photon-to-heat conversion in the winter for lowering the U-factor, and photon-to-electricity in warmer seasons as a solar panel, and (3) the dual modality can be switched easily depending upon the seasonal changes and internal thermal needs. In the wintertime, the photo-thermal effect is utilized to heat the single-pane in order to reduce heat loss. The single-pane is switched to the PV mode in warmer seasons especially in the summer for producing electricity.

The synergetic effects of PT and PV, seasonably alternated, will significantly improve building energy efficiency. In sharp contrast to conventional windows, the

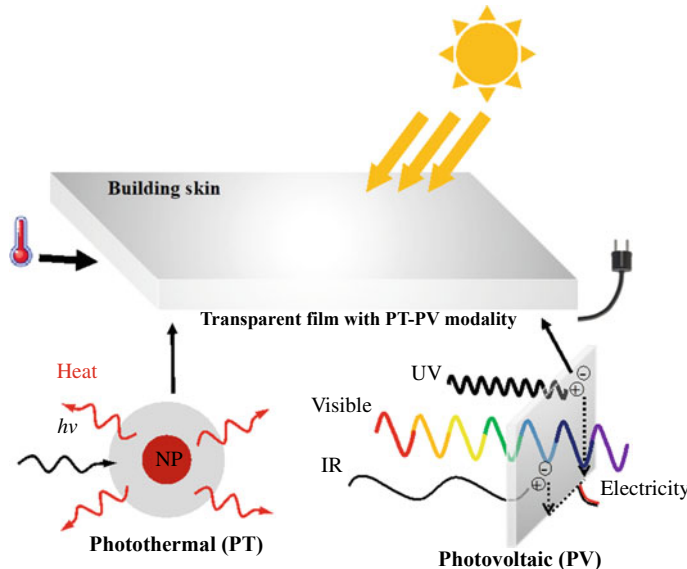


Fig. 1.5 Schematic of PV-PT dual modality building skin

building skin with the PT and PV dual modality will essentially become an energy generator and convertor rather than a source of heat loss. The advantages of this approach are several-folds: (1) no insulating medium is needed as in the traditional double-pane structure; (2) the building skin with the PT-PV thin films can be mass-produced with low cost; (3) the PT-PV thin films can alternatively generate heat and electricity with a much large surface area; (4) ΔT between the warm room interior and the inner window glass surface temperature can be spectrally tuned by adjusting the composition and additives in the PT-PV films, and (5) adhesive products built upon this approach can be applied in wide-scale energy-efficient window retrofits with low balance-of-system costs.

1.1.3 3D Solar Harvesting and Photothermal Energy Generation for Building Heating Utilities

In recent years, formation of megacities presents enormous social and environmental challenges. The sustainability of megacities depends to a large extent on how to manage the energy and material resources. In particular, the use of electricity is not only inefficient but also environmentally detrimental. The combustion of fossil fuels is responsible for the majority of emissions of carbon dioxide CO_2 , sulfur dioxide SO_2 and nitrogen oxides NO_2 (Perera, 2018). To address these critical energy inefficiency issues, utilization of solar energy via PV has been the main approach to

produce clean energy. However, PV requires additional utilities for solar harvesting, electricity generation, storage and distribution, which is not ideal for a net zero energy system. Although the source of energy appears “free” as it is abundant in nature, the processes in harvesting solar light can be quite costly against the net economic gains. It has been estimated that the solar energy costs approximately 8 times more than primary fuels (oil, coal, gas) (Michael, 2021). Furthermore, production of silicon PV panels is not “clean” as the byproduct silicon tetrachloride can be both occupational and environmentally hazardous (Kizer et al., 1984; Are solar panels toxic to the environment, 2021).

Solar heating in buildings is achieved mainly by letting sunlight through windows or guiding it in building structures via optical means such as solar tunnels (solar pipes) (Spacek et al., 2018; Zhang, 2002). From these solar collectors, the heat is transferred by conventional equipment to warm up the living spaces of a building. Although certain solar energy can be harvested and utilized for energy consumption, the energy efficiency has not been satisfactory. Windows and skylights can be classified as conventional passive daylighting devices, and their performances are greatly constrained by the external and internal obstructions. Many conventional equipment requires electricity-driven fans, causing an addition of energy consumption. For instance, heating, ventilation, and air conditioning (HVAC) consume 40% to 50% of the building’s energy, which is mainly supplied by primary fuels (natural gas) (Irace & Brandon, 2017). The current solar technologies are categorized into two types, namely, active solar energy and passive solar energy. The former deals with actively harvesting and concentrating solar energy by various technical means and convert it to other forms of energy such as electricity (PV) (Chang et al., 2018; Chen et al., 2012; Husain et al., 2018; Traverse et al., 2017). The latter relies on daylighting devices including windows, mirrors, prismatic glazing, light shelves, atrium and light pipes for passively collecting sunlight (Irace & Brandon, 2017; Zhang, 2002). The typical active solar space heating involves collectors to absorb solar radiation in either liquid or air. Distributions of heat require either pumps or fans depending upon the heat transfer medium. For passive solar space heating, solar light is harvested mainly through architectural features such as windows, light shelves, atrium and light pipe. Thermal mass materials such as concrete or tile are typically used to absorb heat during the daytime and release it at night. However, these passive solar space heating devices are not sufficient to heat the commercial buildings and not energy-neutral.

For next generation energy-neutral civic structures, a new concept of Energy-Free Photo Thermal System (EFPHS) can be established based on transparent multi-layer photothermal nano coatings (Fig. 1.6). As shown in Fig. 1.6, the solar light is harvested by the dome of a solar-tunnel (solar light collector) and directed through an array of transparent glass substrates coated with a photothermal material. Upon solar irradiation, the photothermal coating can convert photons to heat efficiently, thus raising the surface temperature of these substrates that function as an “energy-free solar radiator.” The entire system uses natural sunlight, requiring no electric power, or any other forms of energy.

The current energy saving strategies heavily rely on thermal insulation that solely depend on glazing technologies and insulating materials, such as double or triple pane

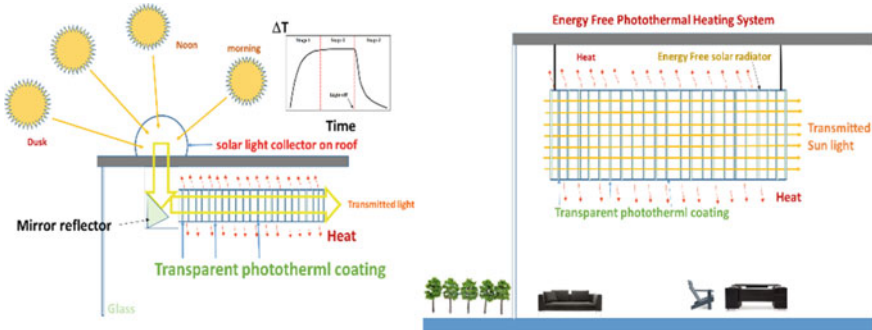


Fig. 1.6 Schematic of Energy-Free Photo Thermal System (EFPHS)

windows. Despite considerable improvements, these approaches are fundamentally incapable of reaching the state of “energy neutral” or “net zero” sustainable systems. The “Energy-Free Photothermal Heating System” (EFPHS) can be structurally and straightforwardly installed in single houses and high-rises as energy free heaters, especially for cold climates. Figure 1.7 shows one of the possible configurations of EFPHS in a building interior. As can be seen in Fig. 1.7, the sunlight is directed from the top, passing through multiple layers of transparent PT films which not only can function as a thermal radiator, but also a light source for building interior lighting. Figure 1.7 is a more realistic illustration of Fig. 1.6.

This chapter will provide the most updated research outcomes on the above topics, namely, (1) optical thermal insulation via photothermal coating of single pane



Fig. 1.7 Installation of a building solar radiator based on the concept of EFPHS

windows, (2) transparent thin film with PT-PV dual modality films for energy efficient building skin, and (3) 3D solar harvesting for generating photothermal energy used in building heating utilities. Novel synthesis routes in making nanoparticles and photothermal solutions will be described in detail with most recent publications. Film deposition methods will also be provided for coating various substrates. These multifunctional hybrid materials and films are characterized with a variety of means including UV-vis spectroscopy for absorption and transmittance, and Raman study for fundamental mechanism of structural interactions responsible for the optical and photothermal properties. Both heating and I-V curves of the films are obtained and correlated to their nano and electronic structures. Important engineering parameters including photothermal conversion efficiency and U-factor are calculated and analyzed under different conditions. Also discussed are roles of nanomaterials in next generation building skins, current challenges in multifunctional designs of large-scale surface energy devices, and future opportunities. Several new concepts are presented with their future energy applications, industrial viabilities, and commercial potentials.

1.2 Photothermal Materials for Energy Efficient Building Skin: Synthesis and Property Characterization

As noted above, the residential and commercial sectors counted for 40% of total U.S. energy consumption in 2020 (How much energy is consumed in U.S. buildings, 2021). The primary heat loss from conventional buildings is from windows since they are poor thermal insulators, which is a particular challenge of energy saving in cold climates. The conventional approach has been applying double- or triple-pane windows for reducing heat loss. However, these glazing technologies cost two to three times more than the single-pane windows (ARPA-E, 2014). To replace double-pane with single-pane, the key issue deals with reducing heat transfer of the window at the same level of the double-pane without any intervening medium. The so-called Optical Thermal Insulation (OTI) was developed by a transparent photothermal coating on the inner surface of the window for raising the surface temperature that is close to the room interior temperature. Note that this window surface heating is solely by solar irradiation, and not requiring any additional electricity, therefore entirely energy neutral.

The photothermal effect is a physical phenomenon relating to conversion of solar light to thermal energy by nanoparticles based on the so-called as localized surface plasmon resonance (LSPR). The photothermal effect of thin films has been extensively investigated for energy applications based on the heat generated by applied electromagnetic radiation in a particular wavelength range. The first photothermal thin film for energy-efficient window applications was reported by Zhao et al. (2017). The concept of the energy-efficient window involves a photothermal thin film coating on the inner surface of the window (Fig. 1.2). The window surface temperature will

increase due to the photothermal effect under solar irradiation. The thermal transmittance of the window depends on the temperature difference (ΔT) between the single-pane and that of the indoor room. The reduction in ΔT effectively lowers heat transfer through the building skin via photothermal heating, characterized by a low U-factor, without double- or triple-glazing.

1.2.1 Synthesis and Characterization of the Photothermal Materials: Porphyrins and Iron Oxides

In the following, detailed synthesis routes are introduced on making a variety of photothermal materials including metals, carbon-based materials, organics and inorganics, iron oxides, and composites. Processing methods include solution synthesis and thin film deposition. Also introduced are nanoparticle techniques such as coprecipitation, hydrothermal synthesis, insert gas condensation, etc.

1.2.1.1 Synthesis of Iron Oxide and Its Composite

One pot coprecipitation synthesis is an efficient method for synthesizing nanoparticles. In our laboratory, we utilized one pot coprecipitation to synthesize photothermal materials, such as Fe_3O_4 and $\text{Fe}_3\text{O}_4@\text{Cu}_{2-x}\text{S}$. These nanoparticles were also modified by coating of poly(acrylic acid) and polystyrene to achieve hydrophilic surfaces (Lin et al., 2020; Tian et al., 2013; Zhao et al., 2017). Specifically, a given amount of oleylamine was heated to 300 °C in a nitrogen environment and stirred. A mixture of Fe (acac)₃ in oleylamine/N-methyl-2-pyrrolidone was injected into a preheated oleylamine. By keeping the solution at 300 °C until the solution was well mixed, the solution was cooled down to 60 °C. Fe_3O_4 nanoparticles were collected by a strong magnet and washed by methanol. The final product was dried by freeze drying. The $\text{Fe}_3\text{O}_4@\text{Cu}_{2-x}\text{S}$ nanoparticles were developed by coating Cu_{2-x}S onto the Fe_3O_4 nanoparticles, forming a core–shell structure. For Cu_{2-x}S coating, a specific amount of Fe_3O_4 nanoparticle solution was heated to 70 °C. A mixture of sulfur in an oleylamine/cyclohexane solution was injected into Fe_3O_4 nanoparticle solution and stirred for 10 min at 70 °C. Subsequently, a mixture of Cu (acac)₂ in an oleylamine/chloroform solution was injected into the reaction system and stirred for 30 min to form $\text{Fe}_3\text{O}_4@\text{Cu}_{2-x}\text{S}$ nanoparticles. $\text{Fe}_3\text{O}_4@\text{Cu}_{2-x}\text{S}$ nanoparticles were collected by a magnet and washed by methanol. The final product was dried and dispersed in toluene for thin film coating.

The mechanism of the photothermal effect has been identified as localized surface plasmon resonance (LSPR). LSPR refers to a surface plasmon confined in a nanoparticle smaller than the incident light wavelength. In contrast with surface plasmon resonance (SPR), LSPR is a particular type of SPR for nanoparticles related to nanoparticles' size and shape. The so-called dipole approximation of Mie theory

describes the nanoparticles' response to the electric field vibration. The size of the scattering particles relative to the light wavelength is described by Mie scattering (Wei et al., 2013; Zaitoun et al., 2001). At plasmonic resonance, the electric fields are enhanced near the particle surface, and this enrichment drops off with distance from the surface. As a result, the optical absorption of the particle is at its maximum at the plasmon resonant frequency. This phenomenon occurs at visible wavelengths for noble metal nanoparticles. The dissipation of LSPR as thermal energy results in temperature increase.

1.2.1.2 Extraction of Chlorophyll

The extraction method of chlorophyll was reported in previous research (Zhao et al., 2019b). Fresh spinach leaves were cut into small pieces (~5 mm × 5 mm) and freeze-dried at -0 °C to dewater. The dried leaves were washed by using petroleum ether to remove the carotenoids and waxes. The chlorophyll can be extracted by immersing the washed leaves in 75% methanol and 25% petroleum ether at room temperature for 24 h. Subsequently, the solution was transferred to a separatory funnel and washed with saturated sodium chloride solution. The organic phase and aqueous phase were then separated by saturated sodium chloride solution. The organic phase was subsequently filtrated and removed by rotary evaporation to obtain the isolated film. The film was dissolved in acetone and stored at -20 °C for at least 24 h to precipitate the remaining impurities. Precipitates were collected by centrifugation, and the isolated chlorophyll was obtained by rotary evaporation. The final product was dissolved in toluene and stored at -20 °C for use.

1.2.1.3 Deposition of Photothermal Thin Films

Spin coating is a procedure used to deposit uniform thin films onto flat substrates. First, a small amount of coating material is applied to the center of the substrate, and then the substrate is rotated at a speed to spread the coating solution by centrifugal force. The liquid will be evaporated during spinning, leading to a uniform film. To form a thin film, the photothermal (PT) material solution is mixed with certain amount of polymer, such as polymethyl methacrylate (PMMA), polyethylene glycol (PEG), polyacrylic acid (PAA), or epoxy resin, etc. The viscosity of the solution can be increased by mixing PT materials with polymer, allowing the thin films to be coated on the glass substrates consistently.

PT materials are dispersed or dissolved in a solvent and mixed with a polymer, resulting in a well-mixed solution. The solution is dropped on the substrate while spinning with a specific speed, time, and amount of solution. Therefore, the spin coating parameters are essential in obtaining high-quality films, and these include spin speed, spin time, amount of materials dropped on the substrate, and the viscosity of the solutions.

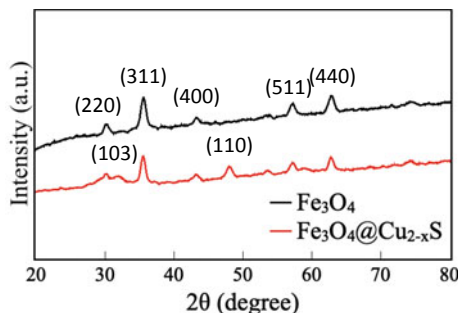
In our spin coating experiments, the Fe_3O_4 and $\text{Fe}_3\text{O}_4@\text{Cu}_{2-x}\text{S}$ nanoparticles were mixed with a certain amount of PMMA in toluene. The mixture was coated evenly on a 25 mm \times 25 mm glass substrate by dropping 100 μL of solution at 2000 rpm for 20 s (Tian et al., 2013). The spinning time or speed has to be optimized for different evaporation rates of the solutions. While water or some nonvolatile (such as epoxy resin) species evaporates much lower, toluene is a highly volatile chemical. Furthermore, sodium copper chlorophyllin can only be well dissolved in water and mixed with PEG (Zhao et al., 2019a). In this respect, the spinning speed will have to increase to 3000 rpm and the spinning time will be extended to 30 s in order to evaporate as much liquid as possible. Different materials require specific solvents, and it is essential to find a compatible polymer and solvent to form the films using the spin processor. Therefore, the spinning time and speed must be well controlled and optimized in the deposition of a variety of PT materials for obtaining uniform and structurally homogeneous films.

1.2.2 Structure and Microstructure of Photothermal Materials

The X-ray powder diffraction (XRD) patterns of both the Fe_3O_4 and $\text{Fe}_3\text{O}_4@\text{Cu}_{2-x}\text{S}$ samples are shown in Fig. 1.8. The X-ray diffraction pattern of the core–shell sample can be indexed as a mixture of the Fe_3O_4 (PDF# 01-1111) and CuS phases (PDF# 01-1281). The diffraction pattern associated with Fe_3O_4 (PDF# 01-1111) are shown in Fig. 1.8. The diffraction peaks at $2\theta = 30.28^\circ, 35.6^\circ, 43.2^\circ, 57.28^\circ$ and 62.9° can be assigned to the (220), (311), (400), (511) and (440) facets of planes of Fe_3O_4 (PDF# 01-1111) (Tian et al., 2013). These results clearly distinguish the formation of Fe_3O_4 from the Fe_2O_3 nanocrystals through the synthesis described above. Notably, the peaks at $2\theta = 31.8^\circ$ and 48.1° represent the (103) and (110) planes of CuS as shown in red line in Fig. 1.8 (Zhao et al., 2009).

Figure 1.9 shows the TEM images of the Fe_3O_4 and $\text{Fe}_3\text{O}_4@\text{Cu}_{2-x}\text{S}$ nanoparticles. As shown in this figure, while the former has an average diameter around 10 nm, the latter is slightly larger about 15 nm. The considerable size increases are

Fig. 1.8 Powder X-ray diffraction patterns of the Fe_3O_4 and $\text{Fe}_3\text{O}_4@\text{Cu}_{2-x}\text{S}$ nanoparticles, as referenced by standard Fe_3O_4 (PDF# 01-1111) and CuS (PDF# 01-1281) phases



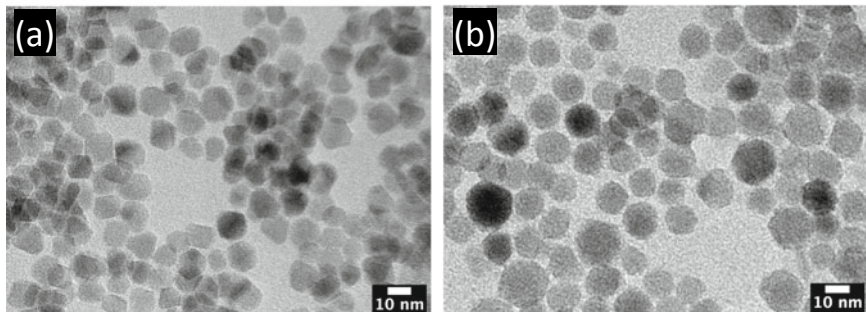


Fig. 1.9 TEM image of **a** Fe_3O_4 nanoparticles and **b** $\text{Fe}_3\text{O}_4@\text{Cu}_{2-x}\text{S}$ nanoparticles

due to the Cu_{2-x}S coating on the Fe_3O_4 nanoparticles, making the microstructures quite uniquely different from a mixture of Fe_3O_4 and Cu_{2-x}S . Furthermore, Fe_3O_4 and $\text{Fe}_3\text{O}_4@\text{Cu}_{2-x}\text{S}$ nanoparticles appear uniform and monodispersed.

The Fe_3O_4 and $\text{Fe}_3\text{O}_4@\text{Cu}_{2-x}\text{S}$ nanoparticles were dispersed in toluene with a given amount of PMMA with good dispersity. The nanoparticle solutions containing both Fe_3O_4 and $\text{Fe}_3\text{O}_4@\text{Cu}_{2-x}\text{S}$ nanoparticles were deposited on glass substrates by using spin coating (Lin et al., 2020). Figure 1.10 shows the scanning electron microscopy (SEM) images of the cross-sectional areas of the films as indicated. As shown in this figure, all thin films exhibit smooth surfaces with varied thicknesses on an average of ~ 500 nm. The thickness differences were caused by various processing parameters such as spinning speed, concentration, solvent, and viscosity (Zhao et al., 2017, 2019a). As shown in Fig. 1.10a and b, the film thicknesses are respectively 464 nm and 497 nm for the Fe_3O_4 and $\text{Fe}_3\text{O}_4@\text{Cu}_{2-x}\text{S}$ thin films with similar morphology and thickness (Zhao et al., 2019a).

Figure 1.10c–f shows SEM images of the chlorophyll, chlorophyllin, hemoglobin, and phthalocyanine films; the film thicknesses are 555 nm, 515 nm, 494 nm, and 442 nm, respectively (Zhao et al., 2017). The surfaces and cross-sections of the thin films play crucial roles in both optical and photothermal properties, which can be further optimized by controlling the amount of precursor solution and spinning speed.

1.2.3 Optical Property Characterization of the Photothermal Thin Films

The spin coated thin films were characterized by using the UV–VIS–NIR spectrometer Lambda 900 (PerkinElmer Inc.) for absorption spectrum. A light transmittance meter (LS116, Linshang, Co. Ltd.) was used to measure the average visible transmittance (AVT).

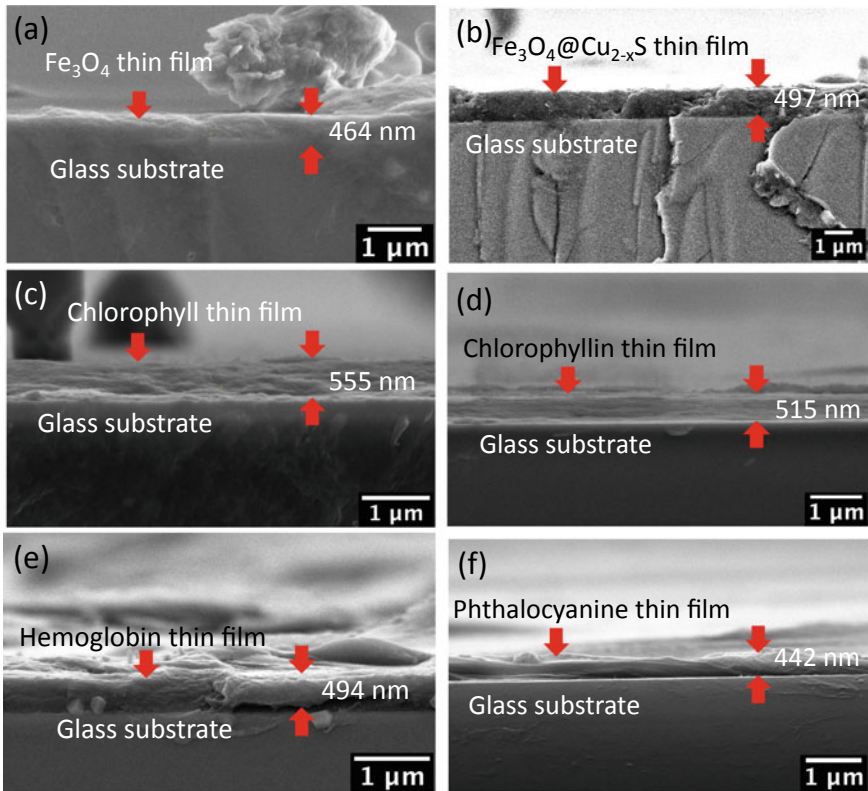
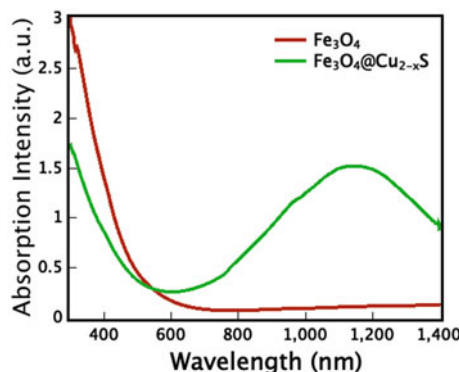


Fig. 1.10 SEM image of cross-section areas of **a** Fe_3O_4 thin film, **b** $\text{Fe}_3\text{O}_4@\text{Cu}_{2-x}\text{S}$ thin film, **c** chlorophyll thin film, **d** chlorophyllin thin film, **e** hemoglobin thin film, and **f** phthalocyanine thin film

Figure 1.11 shows optical absorptions of Fe_3O and $\text{Fe}_3\text{O}_4@\text{Cu}_{2-x}\text{S}$ nanoparticles dispersed in toluene with the identical concentration (0.1 mg/mL). The $\text{Fe}_3\text{O}_4@\text{Cu}_{2-x}\text{S}$ nanoparticle suspension exhibits a broad absorption peak at 1160 nm (green curve), while that of the Fe_3O_4 counterpart presents a similar UV absorption but none in the NIR region. The absorption of the $\text{Fe}_3\text{O}_4@\text{Cu}_{2-x}\text{S}$ solution is characterized with a U-shaped curve which is ideal for window applications. The thin film is highly transparent with an AVT above 90%, and its UV and NIR absorptions can convert photons to heat for raising the window surface temperature in the so-called optical thermal insulation. The NIR absorption of $\text{Fe}_3\text{O}_4@\text{Cu}_{2-x}\text{S}$ nanoparticles is attributed to the Cu_{2-x}S core shell (Tian et al., 2013) due to the LSPR in vacancy doped semiconductors (Zhao et al., 2009).

The absorption and transmittance spectra of the Fe_3O_4 and $\text{Fe}_3\text{O}_4@\text{Cu}_{2-x}\text{S}$ thin films of various concentrations are shown in Fig. 1.12. As shown in this figure, the absorption spectra of the Fe_3O_4 (Fig. 1.12a) and $\text{Fe}_3\text{O}_4@\text{Cu}_{2-x}\text{S}$ (Fig. 1.12c) thin films are consistent with their suspension counterparts. For Fe_3O_4 suspension

Fig. 1.11 Absorption spectra of Fe_3O_4 and $\text{Fe}_3\text{O}_4@\text{Cu}_{2-x}\text{S}$ nanoparticles in solution



and thin films, the absorption intensities diminish beyond 700 nm. Interestingly, the absorption peaks of the $\text{Fe}_3\text{O}_4@\text{Cu}_{2-x}\text{S}$ thin films are red-shifted to 1349 nm, a phenomenon that has been explained by the SPR coupling between the nanoparticles (Kanehara et al., 2009; Lassiter et al., 2008). There are corresponding variations in transmittance for both Fe_3O_4 (Fig. 1.12b) and $\text{Fe}_3\text{O}_4@\text{Cu}_{2-x}\text{S}$ thin films (Fig. 1.12d). With increasing concentration, the AVT of the film is reduced. For comparison, the absorption and transmittance of the control film of pure PMMA are also presented in Fig. 1.12.

Porphyrin compounds are typically characterized with absorptions in the B band (380–500 nm) and Q band (500–750 nm). Figure 1.13 shows the porphyrin compounds of chlorophyll, copper chlorophyllin, hemoglobin, and phthalocyanine in solution forms of the same concentration of 0.01 mg/ml. Chlorophyll, copper chlorophyllin, hemoglobin, and phthalocyanine are dispersed in toluene, water, PBS, and DMSO, respectively. As shown in Fig. 1.13a–c, chlorophyll, chlorophyllin, and phthalocyanine all exhibit saddle like absorptions. Chlorophyll has two main peaks at 413 nm and 668 nm, the corresponding two peaks of chlorophyllin are at 402 nm and 628 nm. Phthalocyanine exhibits a strong peak at 350 nm, and broad absorption in the NIR region with two peaks at 638 nm and 730 nm. Interestingly, hemoglobin presents only one peak near UV at 405 nm, resulting in red color. Spectrally, the colors of these porphyrins vary according to the absorptions through structural replacement of the center atom in the porphyrin ring as can be seen in the porphyrin structures shown in Fig. 1.13.

Figure 1.14 shows absorption and transmittance spectra of porphyrin thin films with different concentrations. The absorption spectra of the porphyrin compound thin films are consistent with their solution counterparts. The absorption peaks are enhanced by increasing the concentration of the materials, while accordingly, the transmittances are suppressed. This figure shows that all porphyrins are quite transparent due to the saddle-like absorptions with broad valleys in the visible region. Note that there is a good correlation between the absorption intensity and the photothermal effect, as shown in Fig. 1.19. The strong absorption enhanced

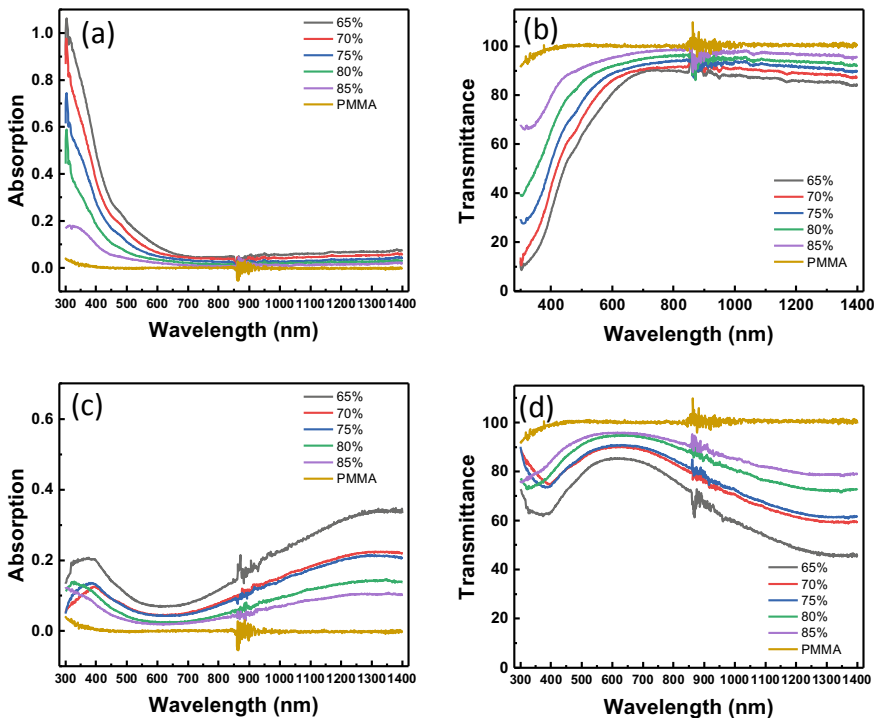


Fig. 1.12 **a** Absorption and **b** transmittance spectra the Fe_3O_4 thin films of various concentrations; **c** Absorption and **d** transmittance spectra of the $\text{Fe}_3\text{O}_4 @ \text{Cu}_{2-x}\text{S}$ thin films of various concentrations

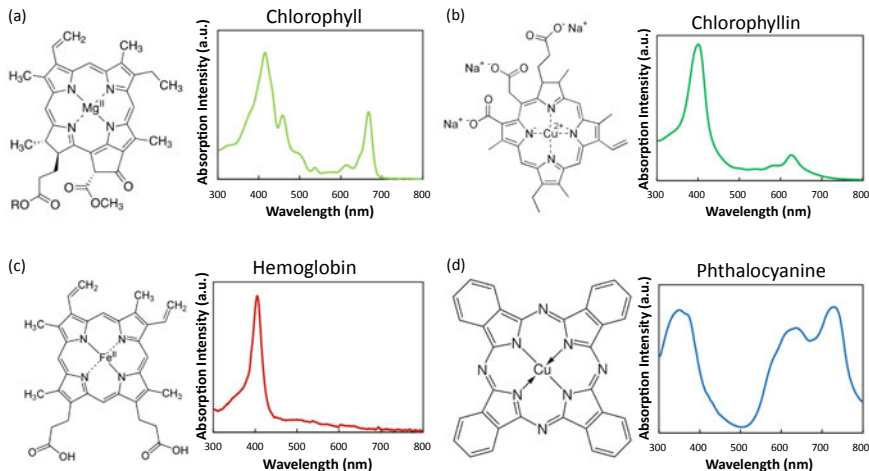


Fig. 1.13 Absorption spectra and molecular structure of **a** chlorophyll, **b** copper chlorophyllin, **c** hemoglobin, and **d** phthalocyanine (Zhao et al., 2019a)

photothermal heating. These thin-film properties are crucial in developing single-panes for window applications: strong UV and NIR absorptions for efficient solar harvesting and thermal energy conversion, but high visible transmittance for window transparency, all characteristically reflected in the saddle-shaped optical spectra.

1.3 Fundamental Studies on the Photonic and Photothermal Mechanisms

1.3.1 Raman Spectroscopy Study

LSPR mainly occurs in metals with high fractions of charge carriers. It was found that porphyrin compounds with much less charge carriers exhibit a different photothermal effect related to the molecular oscillation-induced photothermal effect (MOIPE) based on a Raman spectroscopy study (Zhao et al., 2019a). The Raman spectra of chlorophyll, chlorophyllin, hemoglobin, and phthalocyanine are shown in Fig. 1.15. The excitation laser wavelengths used were 442 nm, 514 nm and 633 nm. The molecular structures interact with the incident EM waves through vibrations of porphyrin ring's phonons and electrons, leading to an energy shift of the scattered photons. As can be seen in Fig. 1.15, the Raman peaks of chlorophyll excited by 442 nm and 514 nm laser are intensified at 1160 and 1540 cm^{-1} (Fig. 1.15a). The Raman peaks represent molecular vibrations of the porphyrin-ring bonds, corresponding to the photon absorptions. Raman scattering can be enhanced when the incident light wavelength is close to the absorption peak of the compound, which is associated with the molecular vibration of the porphyrin specifically, chlorophyll has a strong absorption peak at 413 nm, but no absorption at 514 nm. Therefore, the Raman peaks are well enhanced at 1540 cm^{-1} by the 442 nm laser but not by the 514 nm laser. Consistent results are also obtained from the Raman spectra of chlorophyllin, hemoglobin, and phthalocyanine. For chlorophyllin (Fig. 1.15b), the 422 nm laser excitation is responsible for more intensified Raman peaks at 1370 cm^{-1} and 1580 cm^{-1} . According to the absorption spectrum shown in Fig. 1.15b, chlorophyllin exhibits a stronger absorption at 400 nm, near the 442 nm laser, allowing for much higher Raman peak intensities than those of the 514 nm laser. Furthermore, chlorophyllin is characterized with the highest specific photothermal coefficient for its stronger absorptions near UV and NIR frequencies. The Raman data shown in Fig. 1.15 provides a fundamental base for the photothermal effect associated with the molecular vibrations of the porphyrins.

More evidence for the photothermal effects of porphyrins can be seen from the Raman spectra of hemoglobin and phthalocyanine. The hemoglobin exhibits a strong absorption at 405 nm, giving the Raman peaks greater intensities when excited by 442 nm laser than by 514 nm laser (Fig. 1.15c). However, the Raman scattering behaviors of phthalocyanine are quite different due to wider and stronger absorption above 600 nm (Fig. 1.15d). As expected, the Raman peaks of phthalocyanine are

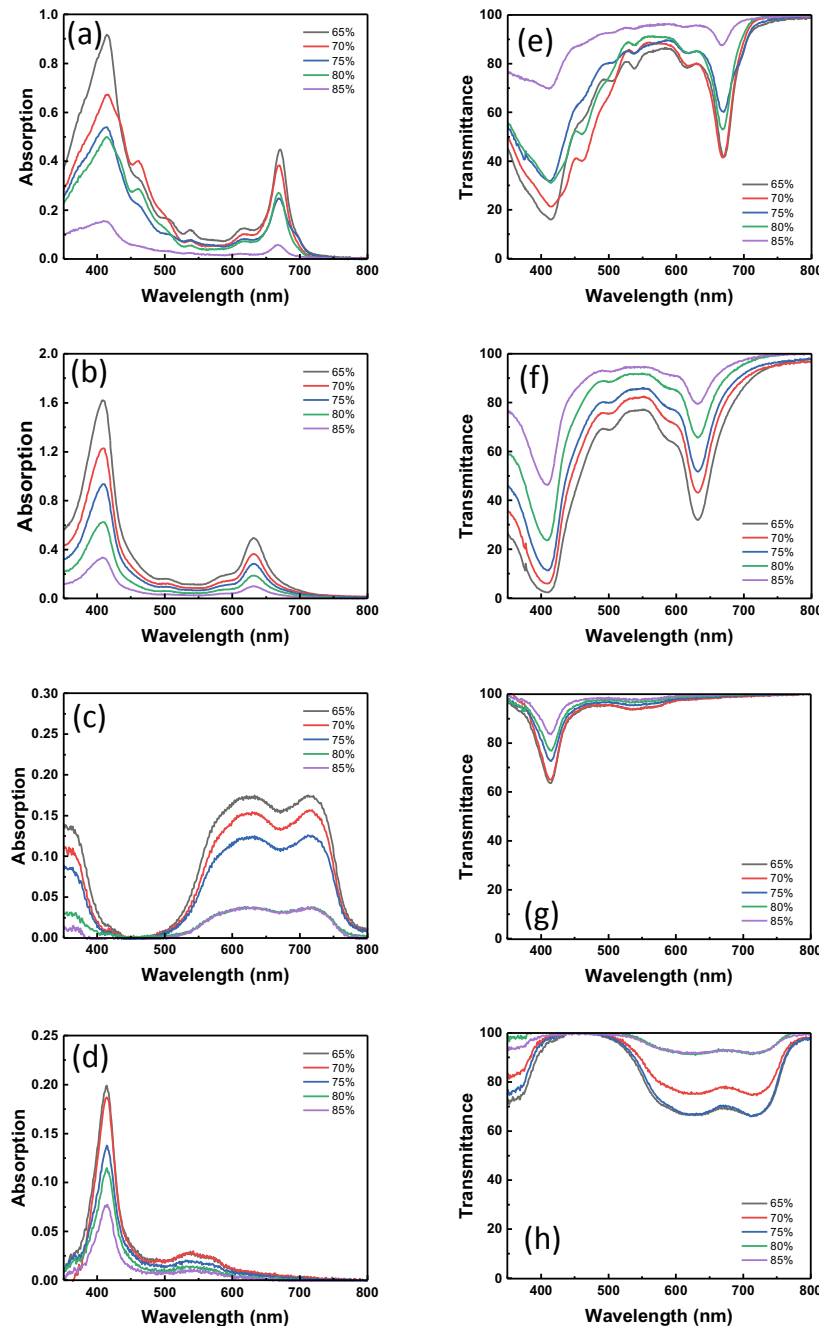


Fig. 1.14 Absorption spectra of **a** chlorophyll, **b** copper chlorophyllin, **c** hemoglobin, **d** phthalocyanine thin films of various concentrations; and transmittance spectra of **e** chlorophyll, **f** copper chlorophyllin, **g** hemoglobin, **h** phthalocyanine thin films of various concentrations

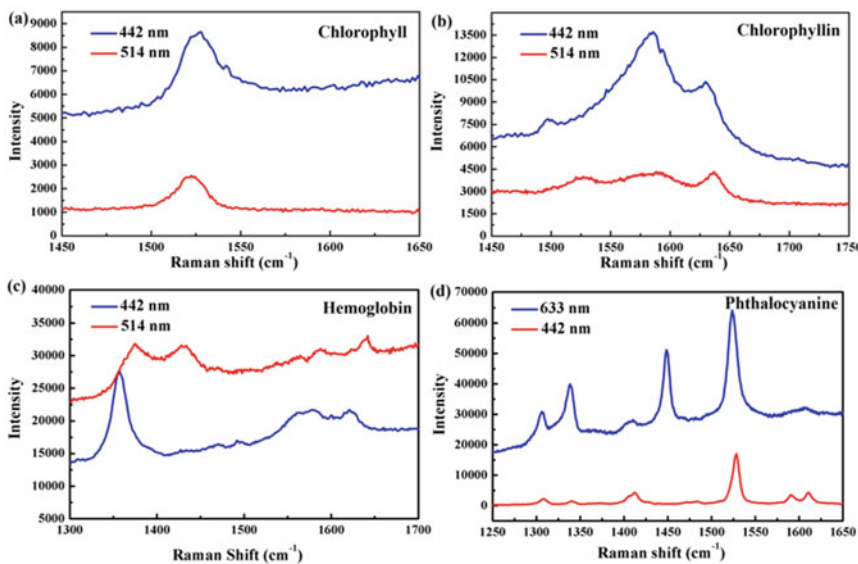


Fig. 1.15 Raman spectra of **a** chlorophyll, **b** chlorophyllin, **c** hemoglobin, and **d** phthalocyanine on aluminum foils by 442, 514, and 633 nm lasers

quite intense by excitation of the 633 nm laser than the 442 nm laser. As evidenced in the Raman spectra of porphyrins (Zhao et al., 2019a), the Raman laser light interactions with the molecular vibration of the porphyrin rings, which are associated with phonons and electrons in the porphyrin structure. These molecular vibrations due to photon excitations can dissipate heat and responsible for the photothermal effects as observed in the heating curves shown in Fig. 1.19.

Within the absorption frequency range, the photon frequency matches the vibration mode of porphyrin and oscillate to generate an electron density distribution. This creates a local electrical field with a dynamically modified charge equilibration (Fig. 1.16). With the constant irradiation by the incident light, the local electrons form a collective oscillation. The collective oscillation dissipates energy in form of heat manifested by the temperature change versus time curves. Porphyrin compounds are semiconductors with limited charge carriers, making LSPR unlikely for the photothermal effect. The molecular vibrations of porphyrins can absorb photons at various frequencies and convert photonic energy to thermal energy, responsible for the photothermal effect.